

Click here to view linked References

Eco-Thermal analysis and response surface optimization of the drying rate of potato slices in a mix-mode solar dryer

Onyenwigwe D.I^a, M. C. Ndukwu ^{a*}, F. I. Abam^b, Ibeh Mathew^b, Ugwu Elijah^a, Akuwueke Leonard^a, Jude Mbanaso^c, Linus Oriaku^d, Hongwei Wu^e, Dirioha Cyprian^a, A.B.Eke^a, Lyes Bennamoun^f

^aDepartment of Agricultural and Bioresources Engineering, Michael Okpara University of Agriculture, Umudike, P.M.B 7267 Umuahia, Abia State, Nigeria

^bExergy, Energy and Environment Research Group (EEERG)Department of Mechanical Engineering Michael Okpara University of Agriculture Umudike

^cDepartment of Agribusiness, Michael Okpara University of Agriculture, Umudike, P.M.B. 7267 Umuahia, Abia State, Nigeria.

^dEngineering Research Unit National Root Crop Research Institute Umudike, Abia State

^eSchool of Physics, Engineering and Computer science, University of Hertfordshire, Hatfield, AL10 9AB, U.K.

^fDepartment of Mechanical Engineering, University of New Brunswick, 15 Dineen Drive, E3B 5A3 Fredericton, New Brunswick, Canada

*Email : ndukwumcu@mouau.edu.ng , Phone : +2348032132924

Abstract

This research aims to establish the interconnectivity between mix-mode solar dryer designs with carbon and energy cost mitigation using different energy scenarios and study the drying kinetics to obtain the optimal drying rates for drying blanched potato slices. This will help the policy makers' in the establishment of design standard for solar dryer fabricators and also assist them in making the right choice for carbon emission management for environmental sustainability and determining the end point of drying potato slices for energy conservation. Hence a mix-mode solar dryer was deployed with sun-drying using blanched potato as a case study. The potato slices were spread on the drying tray to form a thin layer. Mass loss data and Temperature and relative humidity data were recorded at 1 h intervals until the desired moisture content was achieved. The dryer utilized 4.562 M J to dry the potato slices from 64 % w.b initial moisture content to 7.56 % w.b final moisture content. The percentage of the energy utilization ratio (EUR) ranged from 4.19 to 82.68 % with an average value of 39.46% while the thermal efficiency of the solar dry varied from 0.6 % to 34 % with an average value of 17 %. The dryer can save from \$74.22 to \$741.22 per year at a 10 to 100% rate of usage with an indicative payback period of 0.17–1.64 years at the same rate of usage. The decarbonisation potential of the solar dryer was high when compared to coal, diesel or grid electricity-powered dryers as an energy case scenario with the values ranging from 2.9 - 237.71 tones of CO₂ per year with earned carbon credit ranging from \$41.98 to \$ 3446.85 per year. Blanching time affected the drying rate and effective moisture diffusivity of the potato slices with effective moisture diffusivity varying from 6.35×10^{-11} to 7.07×10^{-10} m²/s for sun-dried potato slices and 9.86×10^{-11} to 1.24×10^{-9} m²/s for solar drying potato slices. Using the solar dryer reduced the drying time by 25.81 to 34.48 % compared to open sun drying. The optimum drying rate for the solar-dried untreated potato slices was 0.0239665 kg/h at a collector temperature of 40.93°C and thermal efficiency of 17.30 % while blanching for 3 minutes, 6 minutes and 9 minutes gave optimum drying rate of 0.0177959kg/h, collector temperature (T) of 40.9 °C and thermal efficiency(η) of 17.30 % for the three pre-treatments.

Keywords: Decarbonization, Energy efficiency, blanching, drying rate, optimization

Nomenclature

A	Area (m ²)	Greek letters and symbols
C _p	specific heat capacity (J/kg °C)	σ Standard deviation from a data set.
C	capacity of the dryer per batch (kg/batch)	γ relative humidity of air in the drying chamber (%),
d	drying time per batch (hr/batch)	
E _c	total energy utilized for drying the potato slices (kWh)	
h _c	total heat transfer coefficient (W/m ² K)	
h _{ca}	convective heat transfer coefficient from crop surface to drying chamber (W/m ² K)	ω specific humidity

h_{cb}	Evaporative heat transfer coefficient from crop surface to drying chamber (W/m^2K).	τ	transmittance of the glazing cover
I or I_s	average solar radiation (W/m^2),		
L	latent heat of vaporization of water		
\dot{m}_a	airflow rate (kg/s)	Subscripts	
m_w	mass of water removed (kg)	atm	atmosphere
M	possible mass of potato that could be dried by the dryer per day (kg/day) at full capacity	i	Inlet or initial
N	number of sets	a	air
P_{Tcr}	Partial pressure at crop temperature (N/m^2)	o	outlet
P	Pressure (Pa)	c	collector
P_{Tr}	Partial pressure at drying chamber temperature (N/m^2),	a	Ambient r inlet
R	radius (m)	t	Tray or time
t	Time (h) or (s)	e	equilibrium
T_{cr}	crop surface temperature ($^{\circ}C$),		
T	emperature ($^{\circ}C$)		
T_d	temperature ($^{\circ}C$) of the drying chamber,		
U_o	heat loss coefficient(W/m^2 $^{\circ}C$)		
w	number of days to deploy the dryer and is given as follows		
X or m	Moisture content (w.b)		

1. Introduction

Agricultural products like potatoes at harvest have high initial moisture content, which must be reduced to extend their shelf life for storage, size reduction, transportation, packaging etc. Most times, these products undergo different pre-treatment processes like saline immersion, blanching and laser treatment which activates the enzymes that assist in the moisture removal process and modify the quality of the product after drying. Blanching evacuates air from the cells. It increases the rates of moisture removal while at the same time preventing off-flavour from the dried product (Wang et al., 2018). The most common method for agricultural product drying in Africa is open sun drying (Ndukwu et al., 2020a). In this method, the products are usually spread in a raised platform and continuously watched and manually mixed intermittently until it dries to the desired moisture content (Murthy, 2009). This method poses many problems to the farmers and sellers because of the incursion of animals, dust accumulation, interference from unpleasant weather conditions and colour degradation of green vegetables due to the depletion of chlorophyll by ultra-violet rays from the sun (Jairaj et al., 2009). Additionally, it creates a time management problem for the farmers who have to split their time into going to the farm to tender their crops, monitoring the product being dried and going to the market to sell their product. However, most farmers in developing countries continued to use this method because of the high cost of artificial dryers. Again, drying crops with artificial dryers that use fossil-based energy sources will generate greenhouse gases like carbon dioxide that damages the ecosystem and harm the environment (Ndukwu et al., 2018). These gases also have health implications as they have been revealed to adversely affect human and animal health. Therefore, using artificial dryers is discouraged due to environmental concerns. Thus adopting renewable energy-powered drying equipment has been encouraged. Among these renewable systems, solar thermal systems are becoming popular (Xiong et al., 2021a and 2021 b). Its potential for decarbonization of the ecosystem and cost benefits has been presented in the literature (Ndukwu et al., 2022a, Simo-Tagne et al, 2019). Solar energy is available and well-distributed globally (Ağbulut et al., 2021). Therefore, it has been harnessed and deployed to dry different crops. Solar dryers presented flexibility in designs depending on the size of the enterprises and available material and cost. Thus several studies on the application of solar dryers for crop dryer exist. For example, the thermo-physical properties evolution of red chilli has been studied in a mix-mode solar dryer with sodium sulphate deca-hydrate and sodium chloride as thermal storage by Ndukwu and Bennamoun, (2018). The study obtained a time reduction of 26.7 to 39%. Tellez et al (2018) dried Stevia leaves using direct and indirect solar dryers in a time range of 4 to 10 hours. A pre-treated Cabya fruit was dried to a moisture content of 6 to 9 %wb with a forced conventional indirect solar dryer for 18 h (Hawa et al., 2021). Triple-

1
2
3
4 pass solar air heater with thermal storage has been investigated by Keavan and Arjunan (2018) for drying mints
5 while Yassien et al (2020) integrated nets of tubes below the absorber in their design. Ndukwu et al (2022b) studied
6 the drying kinetics of cocoyam slices with a partitioned single-pass indirect solar dryer. They concluded that the
7 two-term model best predicted the drying kinetics of the sliced cocoyam in the dryer. Arun and Jayaraj (2021)
8 investigated solar drying of bitter guard using an indirect multi-tray solar cabinet dryer for 11 to 12.5 h at different
9 air flow rates. They found a need to re-order the drying trays intermittently to achieve uniform drying. Sekhar et al
10 (2021) dried ginger with a tunnel dryer with thermal storage from an initial moisture content of 82 % to 10 % (w.b)
11 in 14 to 18 h for active and forced convection mode of air conveyance. They concluded the Midili-Kucuk and
12 Wang-Singh models best predicted the drying kinetics of ginger rhizomes. Ndukwu et al (2020a) studied the drying
13 kinetics of plantain chips with a hybrid biomass-assisted solar dryer. Verma et al model was the best-fitted model for
14 predicting the drying kinetics in the solar dryer. Milczarek et al (2017) demonstrated the potential of applying solar
15 thermal energy in prune and tomato pomaces drying using a drum drying set-up. The results showed variable
16 moisture content of the dried product can be achieved as desired for tomato pomace while prune pomace can be
17 dried to 0.18 water activity level, indicating shelf stability. Ndukwu et al (2022 b) presented a novel solar hybrid
18 dryer with paraffin and crankcase oil infused in copper tubing coiled from the collector to the drying chamber as
19 thermal storage to dry ginger rhizomes. The drying efficiency between, the two thermal storage was less than 1.5 %.
20 A mix-mode solar drying of red pepper and grape was carried out by ELkhadraoui et al (2015) and achieved a
21 thermal efficiency of 34 %. Similarly, Azam et al (2020) and Arun et al., (2014) dried tomatoes with a solar
22 greenhouse dryer, obtainin a thermal efficiency of 9.5 and 17.65 %, respectively. It can also observe from the above
23 studies on solar drying of agricultural products that several designs have been presented for drying different types of
24 crops. These include simple cabinet dryers, indirect-type solar dryers, mix-mode solar dryers, forced and natural
25 convection solar dryers etc. Natural convection solar dryers are very simple and cheaper to fabricate; thus the most
26 dominant solar dryer in most developing countries with low electricity penetration density to power the forced
27 convection type (Ndukwu et al., 2020b). Generally, the above studies also showed that the results obtained are
28 affected by the solar dryer design, the product dried and the ambient conditions. Therefore, uunderstanding the
29 drying parameters of agricultural products for different dryer designs and products has always helped dryer
30 fabricators improve the design of dryers. Knowledge of drying kinetics will help determine the end point of drying a
31 particular product to conserve energy and provide information on the evolution of the physical phenomenon and
32 prevention of damage to the product (Corrêa et al., 2010). Determining the optimum drying rate will provide
33 information on the heat and mass transfer process and simulation of drying systems (Correa et al., 2003).

34
35 The United Nations documents stated that energy systems should show the CO₂ emission mitigation
36 potential in the energy mix to elevate renewable energy alternatives and decrease the fossil in the energy mix
37 (Ndukwu et al., 2022c). This will convince policymakers of the impact of fossil energy on the environment and the
38 need to adopt renewable energy alternatives. Therefore, this concept has been developed and incorporated into
39 energy accounting as a carbon credit. This is a set limit for the individual enterprise that must not exceed. However,
40 they can use the carbon credit earned in using renewable energy alternatives to offset that generated by non-
41 renewable energy sources within the enterprise thermal systems. This is to encourage the adoption of renewable
42 energy in the energy mix (Ndukwu et al., 2022c).

43 Furthermore, the cost-benefit of the solar dryer is another environmental tool that can be used to convince
44 crop processors in adopting solar dryer. Therefore the research aims to establish the interconnectivity between
45 natural convection mix-mode solar dryer designs with carbon and energy cost mitigation using different scenarios in
46 the drying of blanched potato slices in Sub – Saharan Africa. The research assessed the economic potential of the
47 mixed solar dryer based on energy cost savings, payback periods and earned carbon credit as well as the drying
48 kinetics of deploying the dryer to dry potato slices. Thus the specific objectives are (1) to study the drying kinetics
49 (drying rates, moisture ratio, diffusivity etc.) of pre-treated potato slices dried with a mix-mode solar dryer (2) to
50 present the optimum drying rate using a response surface approach (3) to present the decarbonization potential of the
51 dryer in terms of earned carbon credit using different energy sources scenario (3) analyze the economic potential and
52 payback periods of drying the pre-treated potatoes using the solar dryer

53 54 **2. Material and methods**

55 56 **2.1 Solar dryer description**

57
58 Figure 2 shows the natural convection mix-mode solar dryer for drying the pre-treated potato slices. The
59 solar dryer is built locally at the engineering workshop of the Department of Agricultural and Bioresources
60 Engineering, Faculty of the Engineering Michael Okpara University of Agriculture Umudike. The dryer is a batch

dryer developed to dry 2 kg of potatoes per batch. The major components of the dryer were the solar collector, the glazing cover, the drying chamber and the chimney. The design specification of the solar dryer is presented in Table 1, while the collector and the drying chamber skeleton were built with hardwood. The collector is a 0.54 m² cuboid-shaped cabinet box force-fitted with galvanized steel sheet, painted black, which serves as the absorber. The collector box is tilted 15.47°N and was covered with a transparent Perspex glass (0.5m²) to allow solar radiation absorption by the collector absorber. The collector box opens into the drying chamber from the base, where heated air from the collector flows into the drying chamber. Inside the drying chamber is fitted five-layer drying trays separated at a vertical distance of 0.01 m from each other. The potato slices are placed on the drying trays during drying. As the hot air impacts the potatoes slices, the air absorbs moisture from the potatoes and escapes through a 0.7 m high galvanized hollow steel chimney centrally fixed at the top of the drying chamber. The drying chamber (0.7 m²) is covered with a 200 μm transparent nylon to allow for direct solar radiation impact on the dried product, thus providing the mix-mode drying condition with hot air flowing from the collector. A door with hinges for loading and unloading the potato slice is fixed on one side of the drying chamber. The drying chamber and the collector are mounted on the wooden stand as shown in Figure 1.



Fig 1: The natural convection mix mode solar dryer showing

Table 1. Design specifications of the natural convection solar dryer

Units	Specifications
Solar collector	Hardwood, tilted 15.47°N, 1.0 1 m x 0.5m x 0. 2m
Absorber	Black painted galvanized metal sheet, 1.0 x 0.5m x 0.001m

Glazing	Transparent glass, 1.0m x 0.5 m, 0.002m
Drying Chamber	Hardwood skeleton. 1m x 0.7m, 45° tapering at 0.3m height at 0.7m from the base
Drying trays	Hardwood skeleton, plastic wire mesh, 0.7m x 0.28m, laid in two's per rack
Polyethene Nylon cover	Transparent, 200µm
Chimney	Hollow galvanized steel, pipe; ϕ 0.75 m and 0.5 m high

2.2 Experimental procedure

Fresh sweet potatoes used for the study were purchased from the local market and sorted for good once. The potatoes were washed and manually peeled with a knife. The initial moisture content of the potato slice was determined using a convective oven (UMB 500 Sehzart, DIN EN 60529-IP 20). The peeled potato was sliced cylindrically to a thickness of 2 mm. The sample slices were separated into four samples and blanched by dipping them in hot water for 3, 6 and 9 minutes in a water bath before rapidly cooling in cold water at room temperature. The fourth sample was not blanched (untreated) and served as a control. Each blanched sample was divided into two and separately dried simultaneously under the sun and in the mix-mode solar dryer. Samples dried in the sun were labelled S₃, S₆, S₉ and S_u while the sample dried in the solar dryer was labelled SD-3, SD-6, SD-9 and SD_u. Drying in the solar dryer and under the sun begins at the appearance of a clear sky at 9.00 am local time and is stopped when the sun sets at 6.00 pm local time. Drying under the sun or the solar dryer was done by spreading the slice on the drying trays to form a single layer on the tray. During the drying, the mass of the potato was recorded with a weighing balance (KERRO model, sensitivity, ± 0.01 g) at one-hour intervals until three consecutive constant weights are achieved. The temperature and relative humidity of the collector and ambient condition were measured at one-hour intervals using the temperature-humidity clock while the drying chamber temperature was measured with a type-k thermocouple connected to a data logger and processed with a laptop computer. The wind speed was measured with a wind vane anemometer while the solar radiation intensity was measured with a pyranometer. The sensitivities, model and manufacturers of the instrumentations deployed in data collection are presented in Table 2.

Table 2: Specifications and sensitivities of measuring instruments

Instruments	Measured Parameter	Specifications	Sensitivity	Manufacturer
pyranometer	Solar radiation intensity	Apogee MP-200, serial 1250,	± 1 W/m ²	APOGEE USA
Digital balance	Mass	KERRO model	± 0.01 g	KERRO, China
Data logger	Temperature and Humidity	HH1147	$\pm 0.1^\circ\text{C}$ and $\pm 1\%$	Omega Stanford U.S.A.
Thermocouple	Temperature and Humidity	K-type, linked	$\pm 0.1^\circ\text{C}$	Omega Stanford U.S.A.
Temperature and humidity clock	Temperature and Humidity	DTH-82	$\pm 0.1^\circ\text{C}$, $\pm 1.0\%$	TLX, Guandong China
Vane anemometer	Wind speed	AM-4826	$\pm 2\%$ of the velocity	Landesk, Guangzhou, China
Hot air oven	Moisture content	UMB 500 Sehzart, DIN EN 60529-IP 20	$\pm 0.1^\circ\text{C}$	Memmert, Germany

2.3 Experimental uncertainties

According to Philip et al (2022), uncertainties occur due to variations in reading values, the type of instrument, the method of calibration and the environmental effects. They stated that the overall uncertainties in experiments are a contribution from both internal and external uncertainties. Most literature considered only the external uncertainties but Philip et al (2022) stated that internal uncertainties are included for very sensitive parameters, especially in solar

thermal systems. Therefore some literatures have included internal and external uncertainties in the overall experimental uncertainty (Kumar et al., 2022; Sansaniwal et al., 2022). To determine the evaluation data, measurement of Temperature, relative humidity; solar radiation intensity and mass of the product were measured. Thus the overall external uncertainties from the measurements are given by Philip et al (2022) as follows

$$U_{\text{ext}} = \sqrt{U_T + U_{\text{rh}} + U_{\text{sol}} + U_m} \quad 1$$

Where U_T , U_{rh} , U_{sol} and, U_m are the uncertainty in the measurement of Temperature, relative humidity, solar radiation and, the mass of the product with their reading errors. For each measurement, the uncertainty (U_x) is given as (Ndukwu et al., 2022b)

$$U_x = \left[\left(\frac{\partial R}{\partial z_1} \right) w_1^2 + \left(\frac{\partial R}{\partial z_2} \right) w_2^2 + \dots + \left(\frac{\partial R}{\partial z_n} \right) w_n^2 \right]^{1/2} \quad 2$$

w_1 , w_2 and w_n are the experimental uncertainty in the variables z_1 , z_2 and z_n .

For Temperature, relative humidity, solar radiation and mass the external uncertainties were calculated as $\pm 0.14\%$, $\pm 0.14\%$, $\pm 1.41\%$ and $\pm 0.11\%$. Thus the overall experimental uncertainty from instrument measurements was determined as $\pm 1.18\%$. The calculated external uncertainties for moisture contents, moisture ratios and energy utilization ratios ratio were $\pm 0.011\%$, $\pm 0.0025\%$ and $\pm 0.0032\%$.

The internal uncertainty for the experiment is calculated according to Philip et al (2022) as follows

$$U_I = \frac{(\sigma_1^2 + \sigma_2^2 + \dots + \sigma_n^2)}{N} \quad 3$$

The percentage of internal uncertainty is given as follows (Philip et al 2022)

$$\% \text{ internal uncertainty} = \frac{U_I}{U_{\text{Imean}}} \times 100 \quad 4$$

Where U_{Imean} is the mean of the total observation. Therefore for Temperature, relative humidity, solar radiation and mass, the percentage of internal uncertainties were 3.8 %, 2.98%, 3.21 % and 1.23%. Thus the total experimental uncertainty for Temperature, relative humidity, solar radiation and mass was 3.94%, 3.12%, 4.62%, and 1.34 %. These values are within the range of total experimental uncertainty reported in the literature for crop solar drying, considering both internal and external experimental uncertainties. Total experimental uncertainty of 4.98 % was reported by Philip et al (2022) for temperature measurement in solar greenhouse dryers while Kumar et al (2022) reported overall experimental uncertainty of 4.12 to 4.36 %.

2.4 Energy analysis

The energy utilized (W) by the solar collector for drying involves energy input from the solar collector and direct solar radiations given as follows (Tiwari and Tiwari 2017)

$$Q_T = Q_u + Q_r \quad 5$$

Where Q_T is the total energy consumed (W), Q_u is the energy input from the collector (W) and Q_r is the energy from direct solar radiation (W). The energy input from solar the solar collector is calculated as follows (Ndukwu et al., 2017)

$$Q_u = A_c F_R [I\tau - U_o(T_c - T_a)] \quad 6$$

U_o is the heat loss coefficient(W/m² °C) deduced from Duffie and Beckman, (2006) as follows

$$U_o = \frac{I(\tau\alpha)}{T_c - T_a} \quad 7$$

F.R. is the heat removal factor given as follows (Lamrani et al., 2022)

$$F_R = \frac{\dot{m}_a c_{p,a}}{A_c U_o} \left[1 - e^{-\frac{A_c U_o F_f}{\dot{m}_a c_{p,a}}} \right] = \frac{\eta_{t\Box}}{[\tau\alpha - U_o \frac{T_i - T_a}{I_c}]}$$
 8

Where α is the absorptivity of the black surface absorber of the collector, taken as 0.90, and τ is the transmittance of glass, taken as 0.9 by assuming the collector cover is transparent (Tiwari and Tiwari 2017).

The heat contribution from direct solar radiation per hour was calculated following the method used by Tiwari and Tiwari (2017) as presented in equations 9 to 14 as follows

$$Q_r = h_c A_t (T_{cr} - T_d)$$
 9

$$h_c = h_{ca} + h_{cb}$$
 10

$$h_{ca} = 2.8 + 3v$$
 11

Where v is the air velocity (m/s)

$$h_{cb} = \frac{0.01667 h_{ca} (P_{T_{cr}} - \gamma P_{Tr})}{(T_{cr} - T_d)}$$
 12

$$P_{T_{cr}} = \exp \left(25.317 - \left(\frac{5144}{(273 + T_{cr})} \right) \right)$$
 13

$$P_{Tr} = \exp \left(25.317 - \left(\frac{5144}{(273 + T_r)} \right) \right)$$
 14

The solar collector thermal efficiency is determined as follows (Lamrani et al., 2022)

$$\eta_{th} = \frac{\dot{m} c_{p,a} (T_c - T_a)}{Q_u}$$
 15

The energy utilization ratio (E.U.R.) can be used for the energy assessment of the solar dryer. It is the ratio of the instantaneous energy required to convert all the water in the dried potato slice to steam which can show the effectiveness of the energy utilization. It is given by Caesar et al (2021) as follows

$$EUR = \frac{m_w L}{I_s A_c + \dot{m}_a c_{p,a} \Delta T}$$
 16

Where m_w is the mass of water removed calculated due to evaporation (Ndukwu et al., 2022d)

$$m_w = (\omega_i - \omega_o) \dot{m}_a$$
 17

To determine the value of the specific humidity, equation 9 is used as follows (Nugent et al., 2019).

$$\omega = \frac{\epsilon \cdot P_v}{P_{atm} - P_v \cdot (1 - \epsilon)}$$
 18

ϵ is the ratio of a gas constant between wet and dry air taken as 0.622 kg kg⁻¹, and P_v is the vapour pressure calculated as follows (Nugent et al., 2019).

$$P_v = 610.8 \exp \left(\frac{17.27 T}{T + 273} \right)$$
 19

2.5 Environmental impact assessment of the solar dryer

The environmental impact of using the natural convection solar dryer was assessed based on the CO₂ prevention potential of the solar dryer. The dryer was assumed to dry about 20 kg of potato slices at full capacity. Several

methods are used to determine the CO₂ mitigation potential. In this case, we considered three possible sources of energy (diesel, electricity and coal) for artificial dryers and equate the energy utilization of the solar dryers to them. For a diesel-powered dryer, the energy utilized in kWh can be deduced according to Ndukwu et al. (2017) as follows

$$Q_T = v_d k_d \eta_d \quad 20$$

Where Q_T is the total energy utilized in drying the potato slices at full capacity, η_d is the efficiency (taken as 30 %) of the diesel generator, k_d (10.08 kWh/L) is the heating value of diesel, and v_d is the utilized volume of diesel (L) to produce the energy utilized.

Combining equations 5 and 20, the volume of the diesel (v_d) that can produce the equivalent energy is deduced. Therefore, the mass of CO₂ mitigated from entering the atmosphere is determined as follows (Ndukwu et al. (2017)

$$m_{CO_2} = v_d k_f \quad 21$$

The k_f is a constant given by Oudrech et al (2012) as 2.63 kg/L

For an electricity-powered dryer the mitigated mass of CO₂ is determined as follows (Simo-Tagne et al., 2019)

$$M_{CO_2} = EF_{CO_2} \times Q_u \quad 22$$

Where EF_{CO_2} is the countries emission factor which is 0.4392 kg of CO₂/kWh for Nigeria

To compare the energy consumed to dry in the solar and coal-fired dryers to determine the mitigated CO₂, equation 11 is used as follows (Simo- Tagne et al 2019)

$$M_{CO_2} = \sum_i f_i \left(\frac{f_{es} Q_d Q_u}{\eta_i} \right) EF_{CO_2} \cdot F. C. O_2 \left(\frac{44}{12} \right) \quad 23$$

Where FCO_2 is the equivalent fraction of CO₂, given as 0.9, f_i is the fraction of solar potato dried taken as 1.0, η_i is the solar collector efficiency, Q_d is the mass (kg) of sliced potato dried Q_u is the energy consumed by the solar dryer for drying (M.J.). $EF_{CO_2} = 0.0258$ kg/M.J.; $f_{es} = 1$.

2.6 Earned Carbon credit

One of the benefits of solar dryers is the atmospheric mitigation of carbon dioxide which might have been produced if fossil fuel is burnt to produce equivalent input energy from the collector to dry the same quantity of product. To elevate the importance of renewable energy in the energy mix, the solar dryer should be seen to cut down considerably the amount of greenhouse gas in the environment. These can be quantified monetarily as earned carbon credit. Thus we show this advantage in equation 24 (Alic et al., 2021) for indicative purposes we consider emission from coal-generated electricity with an approximate emission rate (k) of 0.98 kg/kWh (Singh and Gaur, 2021) as follows.

$$zCO_2 = zCO_2 \times M_{CO_2} \quad 24$$

Where zCO_2 is the global price of carbon dioxide given as \$14.5per ton (Yousef and Hassan, 2020), M_{CO_2} is the annual mass of CO₂ emission (ton) (Alic et al., 2021)

2.7 Cost analysis based on energy utilization

The economic analysis is deduced bearing in mind that solar dryers are intermittent in use and the available sunshine hours vary from one location to another. Therefore the amount of money that could be saved by using the solar dryer will also vary based on the rate of usage. Thus the amount of savings is determined as follows (Herez et al. 2017)

$$S_1 = u \cdot E_{cyr} \cdot E_{price} \quad 25$$

Where u is the rate of usage graduated in percentage from 10 to 100% (0.1 to 1.0), E_{price} is the country's energy cost per kWh which is taken as 0.057\$ per kWh for Nigeria. The total energy consumed (E_{cyr}) per kWh per year is given as follows (Herez et al. 2017).

$$E_{cyr} = E_c \cdot w \cdot 12 \quad 26$$

$$E_c = Q_T \times t \quad 27$$

Where Q_T is the total energy consumed (kW) to dry, t is the total possible time (h) the dryer could be deployed per day given as follows (El Hage et al., 2018)

$$t = \frac{M}{c} \times d \quad 28$$

The dryer can dry 20 kg of potato per day for a single batch of 20 kg/batch at full capacity in about 20 h.

Therefore, the payback period (PBP), is determined as follows (G.P.P., 2022) as follows

$$PBP = \frac{\ln\left(1 - \frac{C_c}{S_I}(d-i)\right)}{\ln\left(\frac{1+i}{1+d}\right)} \quad 29$$

Where C_c is the capital cost of the dryer, d is the interest rate on long-term investment (11.5%) and i is the inflation rate (15.70 %) for Nigeria.

2.8 Drying kinetics and response surface optimization

The content of the potatoes cylinders was calculated as follows (Ihediwa et al., 2022)

$$X_t = X_i - \frac{X - X_t}{X_i} \quad 30$$

The drying rate is determined as follows (Ihediwa et al., 2022)

$$dr = \frac{m_t - m_{t+\Delta t}}{\Delta t} \quad 31$$

The optimum response of the drying rate to collector temperature and collector efficiency was determined using the Response Surface Methodology (R.S.M.) tool. Valarmathi et al, 2017 and Ihediwa et al (2022) have established that R.S.M. which is an empirical optimization technique can be used to determine the optimum response of the input variables, using the statistical data as shown in equation 32

$$Z = f(b_1, b_2, \dots, b_m) + \varepsilon \quad 32$$

Where Z is the response variable and $b_1, b_2 \dots b_m$ are the independent variables and ε is the residual error. The obtained results were subjected to analysis of Variance (ANOVA) and the best regression equation linking the drying rate for each treatment was determined based on the highest coefficient of determination and the desirability index was used to choose the optimum drying rate responses using design expert 13.

2.9 Mathematical modelling

The experimental moisture content obtained from weight loss was converted to moisture ratio according to equation 33 (Lamrani et al 2022).

$$MR = \frac{X_t - X_e}{X_i - X_e} \quad 33$$

However, according to Lamrani et al (2022) and Ndukwu et al (2010) equation, 33 can be converted to equation 34 when the equilibrium moisture content is small compared to the initial moisture content.

$$MR = \frac{X_t}{X_i} \quad 34$$

To model the drying curve of the blanched sweet potatoes dried in the solar dryer and under the sun, five semi-theoretical thin layer equations as shown in Table 3 were fitted into the moisture ratio data using curve expert software. The best-fit equation was selected based on the highest coefficient of determination (R^2), lowest root mean square error (RMSE) and lowest chi-square(χ^2)

Table 3: Semi-theoretical models for the drying kinetic models

Model name	Model	Reference
Wang and Singh	$MR = 1 + at + bt^2$	Lamrani et al (2022)
Page	$MR = \exp(-kt)$	Lamrani et al (2022)
Logarithmic model	$MR = ae^{-kt} + c$	Lamrani et al (2022)
Henderson and Pabis's	$MR = ae^{-kt}$	Lamrani et al (2022)
Allometric 2 power function	$MR = a + bt^c$	new

2.10 Determination of the variation in moisture diffusivity

Ndukwu et al (2022 c) presented the variation of moisture ratio considering effective moisture diffusivity using the Fourier number (Fo) in equation 35 to 37 as follows

$$MR = \frac{m - m_e}{m_o - m_e} = \exp(-\pi^2 \cdot Fo^a) \quad 35$$

$$Fo = \frac{D_{eff} \cdot t}{R^2} \quad 36$$

Where a is a correction factor given as 0.83, R is the radius (m) of the potato slice

Solving equations 35 and 36, Ndukwu et al (2022 c) gave the moisture diffusivity (D_{eff}) as follows

$$D_{eff} = \frac{R^2}{\pi^{(2/a)} t} (-\ln(MR))^{1/a} \quad 37$$

3.0 Results and discussion

3.1 solar dryer performance

Figure 2 and 3 shows the variation in climatic and solar dryer conditions during the test periods for three days. The maximum radiation intensity achieved was 644W/m² on the first day while the corresponding values were 626 and 487 W/m² on the second and third day respectively. Conversely, the minimum solar intensity was usually recorded in the morning and the evening as the sun sets and these values ranged from 25 to 54 W/m². According to Ndukwu et al., (2017), these values cannot drive the drying process but they can be used to warm up the dryer in the morning especially. However, the average value of the solar intensity was 328.15 W/m² for the three days drying periods. The maximum ambient Temperature of 46.4°C was observed on the first day of drying while the lowest recorded

ambient Temperature was 20.4°C on the morning of the third day. Thus the obtained collector and drying chamber temperatures ranged from 22 to 59.4 and 21 to 56.3 °C, respectively. This value is higher than the ambient Temperature in the range of 1.6 to 13°C for the solar collector and 0.6 to 9.9°C for the drying chamber. The higher Temperature in the collector is because of the absorber and the collector trapping the solar heat within the box before being conveyed into the drying chamber by the moving air. However, higher temperature collector temperature in natural convective indirect solar dryers is not an indication of efficient drying. This is because due to low air speed in the drying chamber, thermal stratification creates a non-homogenous temperature and hinders efficient heat and mass transfer process (Tellez et al., 2018). This is one of the disadvantages of natural convection indirect solar dryers. However, with a natural convection mix-mode design, the Temperature built up in the drying chamber depends not only on hot air flowing from the collector alone but also on the direct solar impact on the dried product. Generally, the relative humidity was low during the drying periods, as shown in Figure 3. The values ranged from 29 to 52% for the ambient and 6.7 to 51.4% for the collector, with an average value of 16.59 – 27 %.

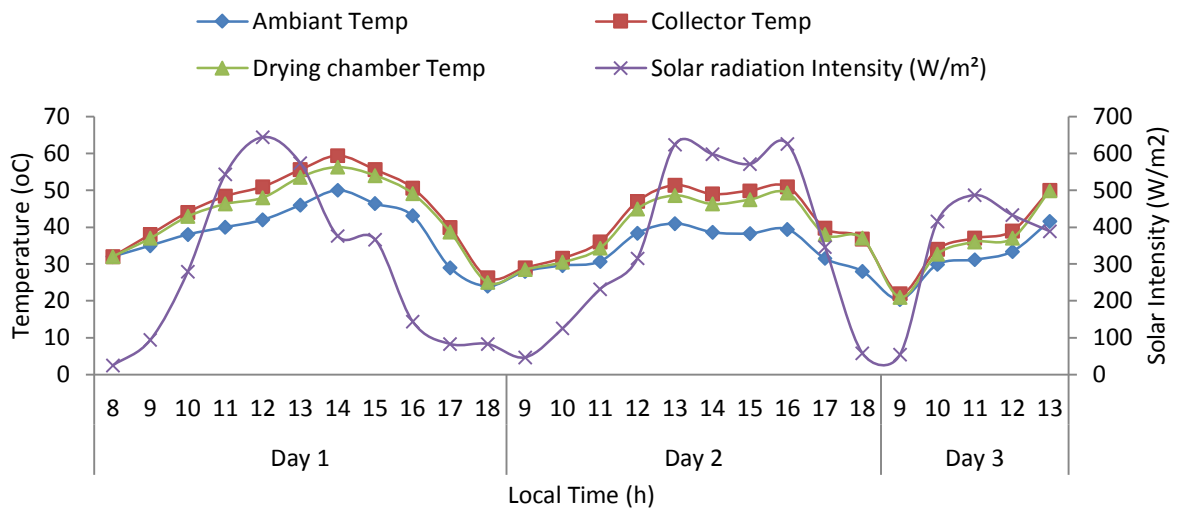


Figure 2: Daily Evolution of Temperature and solar intensity

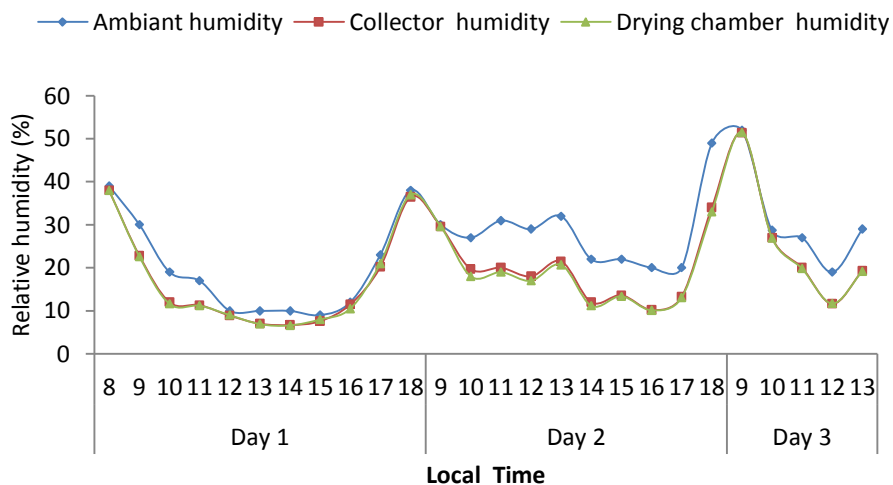


Figure 3: Daily Evolution of Relative humidity

3.2 Energy efficiency analysis

The total average energy input to dry the pre-treated potato is calculated as 6.502 MJ. This represents 29.83 % from direct solar energy into the drying chamber and 70.17 % from the energy input from the collector. However, the effectiveness of energy utilization is determined by the dryer's thermal or energy efficiency, which is the ratio of the energy input to the energy output of the solar collector. In the present study, the average thermal efficiency is 17 %. However, the thermal efficiency varied with time due to weather flux reaching a maximum value of 34 % with a minimum value of 0.6% as shown in Figure 4. Comparatively, in literature, this value falls within the range of some other similar solar thermal systems. Elkhadraoui et al (2015) got a thermal efficiency of 34 % for a mix-mode red pepper and grape drying while Arun et al (2014) got a thermal efficiency of 9.5 % for solar drying of tomatoes in a solar tunnel dryer. Similarly, Azam et al (2020) deduced a solar thermal efficiency of 17.65 % for natural convection solar drying of tomatoes and grapes while Philip et al (2022) obtained an energy efficiency of 17.07 % for drying bitter gourd, tomato and carrot. This showed that the solar dryer presented is among high-performance solar dryers. Furthermore, the solar dryer's energy utilization ratio (E.U.R.) was studied as a parameter for the performance evaluation of the solar dryer. It is a measure of effective heat input conversion in the drying process. It depends on the product's moisture extraction rate and the collector's heat input. Figure 5 shows the E.U.R. flux as the product dries at various drying times. The percentage of E.U.R. varied from 4.19 to 82.68 % with an average value of 39.46%.

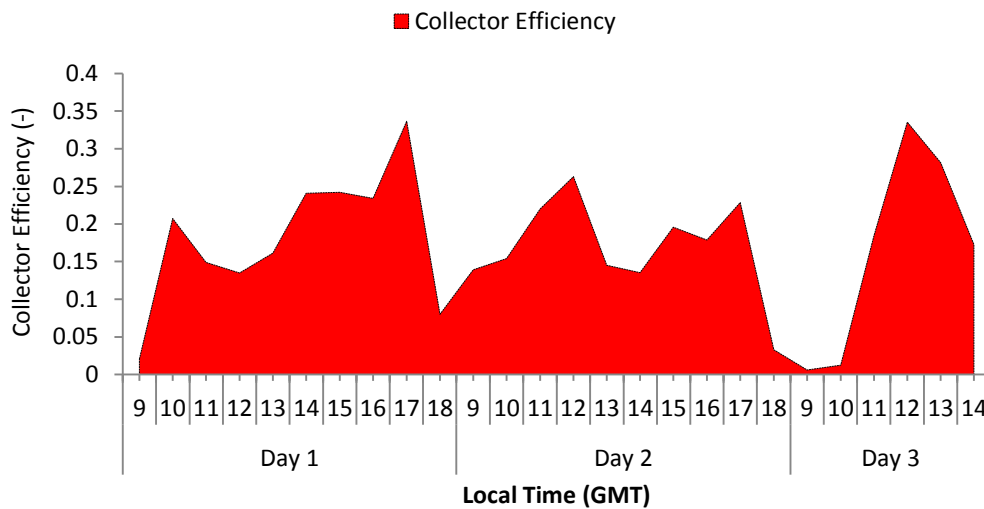


Figure 4: Variation in collector efficiency for the solar dryer

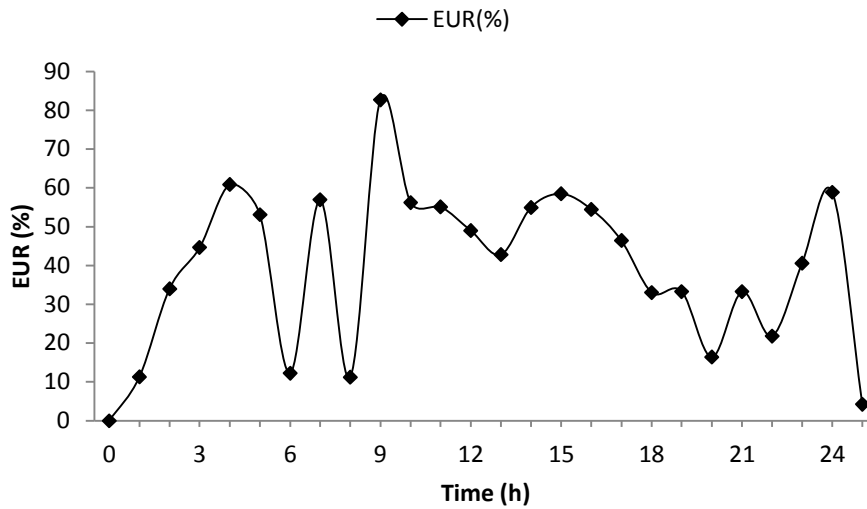


Figure 5: Variation in moisture loss rate for the solar dryer

3.3 Decarbonization potential and earned carbon credit of the solar dryer

The ever-increasing global energy demand with the consciousness of the negative environmental impact caused by high carbon emissions has aroused global interest in cheap, alternative and renewable energy systems. The performance of a renewable energy system should not only base on the efficiency of the system. Still, it must be able to cut down the carbon emission to the environment. Thus, there is a global need for technologies that substantially decarbonize the ecosystem (Rao and Datta, 2020). The earned carbon credit gives a cost overview of the impact of carbon emissions and savings that could be made in terms of cost by deploying solar dryers instead of fossil-based dryers. Therefore the decarbonization capabilities of the solar dryer with consideration of three types of energy input scenarios for a typical commercial dryer for Nigerian conditions were evaluated. The results showed that using the solar dryer instead of fossil-based coal as energy input will limit 237.73 tonnes of CO₂ per year into the atmosphere, while using a diesel-powered dryer will mitigate 5.73 tonnes of CO₂ per year for using the solar dryer, as shown in Figure 6. Additionally, using grid-based electricity will mitigate the lowest amount of CO₂ at about 2.9 tonnes of CO₂ per year. Thus, when this CO₂ is quantified in terms of carbon credit, the amount deducted ranged from \$41.98 to \$ 3446.85 per year, which could be saved if the evaluated solar dryer is used instead of coal, diesel or electric-powered dryers. The results showed coal as the worst emitter while electricity powered dryer is the least comparatively. The obtained result is for the indicative purpose to give an overview of the positive environmental impact of using natural convection solar dryers instead of other energy sources to dry

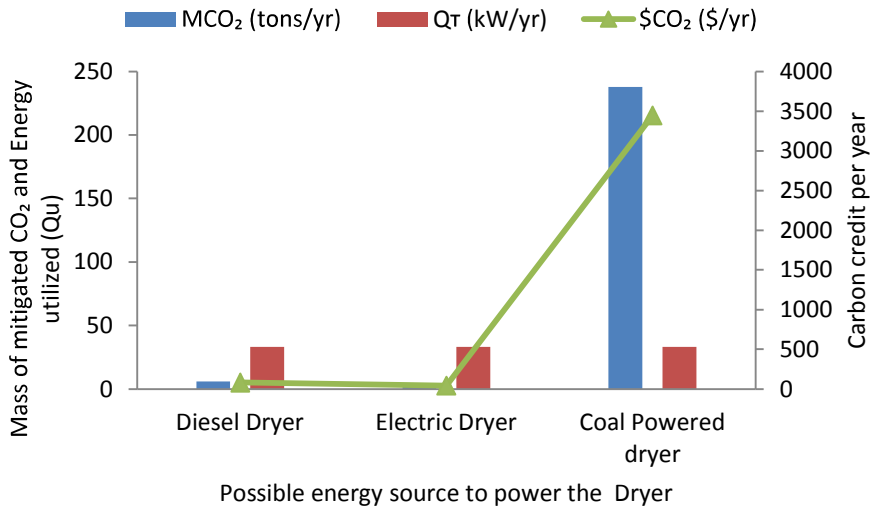


Figure 6: CO₂ mitigation potential of the solar dryer

3.4 Economic assessment of using the solar dryer

To bring home the benefit of solar dryers it is important to provide an indicative cost analysis for using the solar dryer. In this analysis, we assumed a twenty days working period for the solar dryer in a month. Again we graduated the deployment of the solar dryer based on the percentage periods it could be deployed in a month. It is believed that solar dryers are subjected to weather variation and some periods of the day might not be favourable for any meaningful drying. Hence the cost analysis is determined from 10% to 100% rate of usage. Based on this, the cost-saving potential and the payback periods of using the dryer were determined and presented in Figure 7. Payback is critical to making the economic decision to adopt the solar dryer. Thus, short payback time, connotes less risk and high project liquidity (Ndukwu and Manuwa, 2015). The graph shows that the cost saving increased with usage while the payback period decreased. The amount of money that can be saved by using the natural convection solar dryer increased from \$74.22 to \$741.22 as the usage increased from 10 to 100%. At his cost savings, the payback period decreased from 1.64 years to 0.17 years. This means that if the useful life of the dryer goes beyond 2 years, no matter the rate of use the solar dryer will operate almost cost-free of the initial investment cost.

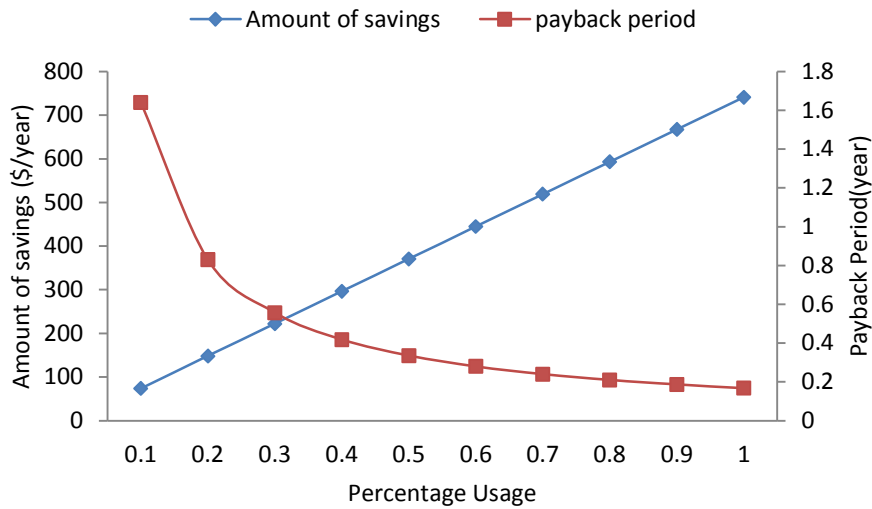


Figure 7: Payback periods and equivalent money saved due to the percentage rate of usage for the solar dryer

3.5 Drying kinetics

3.5.1 Drying rate optimization

The evolution of moisture loss during the drying process is embodied in the drying kinetics. It shows the relationship between moisture loss and different operational variables during the drying process. Figures 8a and 8 b show the moisture loss profile for sun and solar drying of the potato slices. The figure showed a falling rate drying process without constant rate drying periods. This is because the initial moisture content is less than the critical value, therefore, the moisture loss characteristic curve showed an exponential decrease immediately after the moisture loss commenced (Ndukwu et al., 2010). The obtained final moisture content of the dried potatoes was $7.85 \pm 0.64\%$ w.b and it took about 20 to 25 h to achieve this with a solar dryer and 29 to 31 h for sun drying. The drying rate and moisture loss curves showed that pre-treatments affected the drying rate of the potatoes. Other researchers have also reported this on the drying of blanched products (Hawa et al. 2021). Thus blanching for 9 minutes has the highest average drying rate of 1.0184×10^{-1} kg/h, while the lowest was for untreated potato slices with an average drying rate of 9.66×10^{-2} kg/h for sun-dried potatoes slices while it was 1.667×10^{-1} kg/h for drying 9 minutes pre-treated potato in the solar dryer and 1.5191×10^{-1} kg/h for untreated potatoes slices. However, the sinusoidal nature of the drying rate curves in Figures 9 and 10 showed the influence of weather condition fluctuation during the drying process. This is because the intermittent solar radiation leads to non-homogenous temperature variation in the collector and drying chamber, affecting the heat impact on the dried product. Karthikeyan and Murugavelh (2018) and Nukulwar and Tungikar (2021) have obtained a similar graph in solar drying of turmeric using a mix-mode solar dryer and solar cabinet dryer respectively. The drying rates were higher at the beginning due to a rapid temperature rise; however, surface cooling due to moisture evaporation lowers the drying rate as the drying progresses (Philp et al., 2022). A response surface optimization technique was applied at a 95 % confidence limit to determine the optimum responses of drying rate to collector temperature and thermal efficiency of the solar drying of the potato cylinders. Design Expert 13 software was employed and a 3D surface plot of the effect of the drying temperature and thermal efficiency on the drying rate of solar drying of potato slices is presented in Figure 11 The 3D surface plot of the drying scenarios for all the drying pre-treatments showed a non-linear relationship for the three parameters with R^2 value ranging from 0.6149 to 0.896. This is because of the vagaries of weather which affect the ambient conditions. However, the optimum equations and coefficient of determinations for the three pre-treated (SD-3, SD-6 and SD-9) and untreated (un-blanched) potato cylinder is presented in equations 38 - 41 for untreated, blanching for 3, 6 and 9 minutes in that order. The optimum drying rate for the untreated was 0.0239665 kg/h at a collector temperature of 40.93°C and collector efficiency of 17.30 % while blanching for 3 minutes, 6 minutes and 9 minutes gave optimum drying rate of 0.0177959kg/h, collector temperature (T) of 40.9 °C thermal efficiency(η) of 17.30 % for the three pre-treatments.

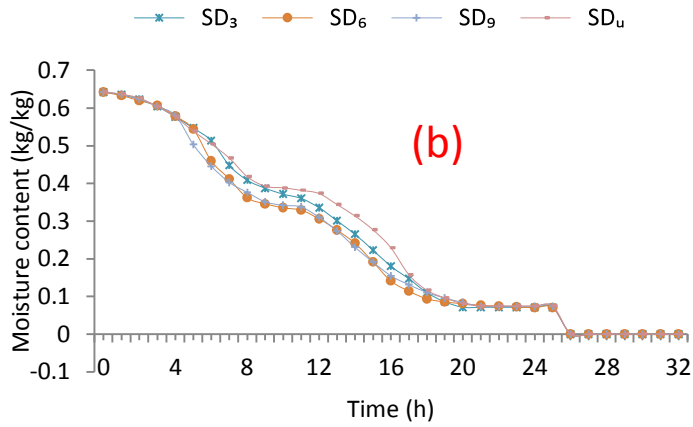
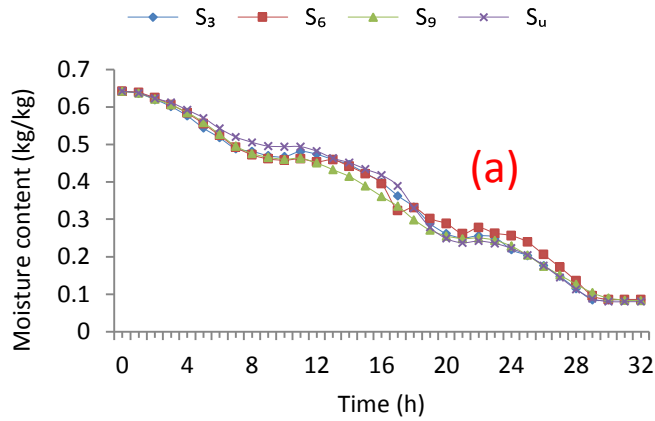


Figure 8: Evolution of moisture content for drying un-blanced and blanced potato slices (a) S- Sun drying (b) S.D.- solar drying, u-untreated sample, and numbers indicate blanching time

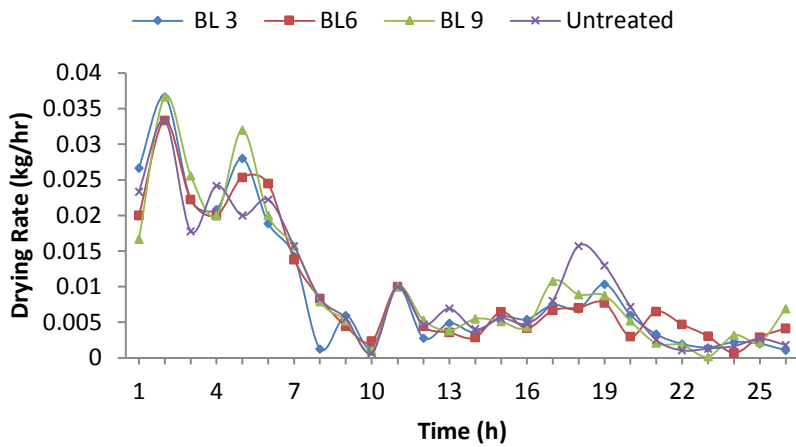


Figure 9: Evolution of the drying rate for sun-dried potato slices with the number indicating blanching time

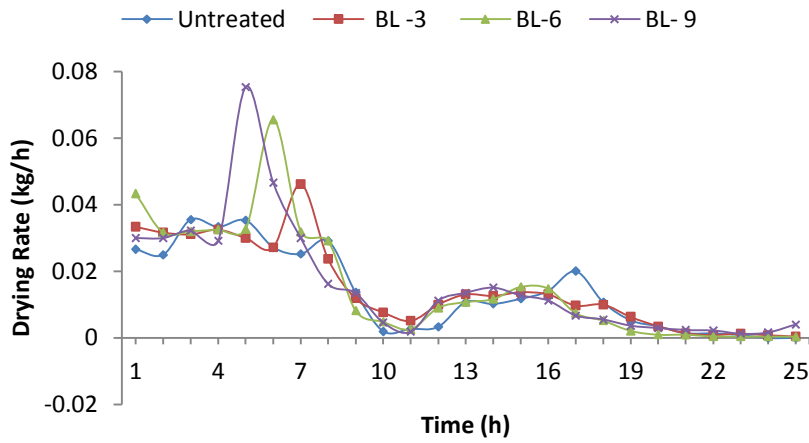


Figure 10: Evolution of the drying rate for solar-dried potato slices with the number indicating blanching time

$dr = 2.4 \times 10^{-2} - 1.4 \times 10^{-3}\eta - 9 \times 10^{-3}T - 1.2 \times 10^{-3}\eta T - 1.96 \times 10^{-2}\eta^2 + 1.8 \times 10^{-3}T^2$	$R^2 = 0.896$	38
$dr = 1.78 \times 10^{-2} + 1.62 \times 10^{-2}\eta - 3.1 \times 10^{-3}T - 2.8 \times 10^{-3}\eta T - 3.3 \times 10^{-3}\eta^2 + 2.6 \times 10^{-3}T^2$	$R^2 = 0.7867$	39
$dr = 1.78 \times 10^{-2} + 1.39 \times 10^{-2}\eta + 6.1 \times 10^{-3}T + 8.3 \times 10^{-3}\eta T - 1.4 \times 10^{-2}\eta^2 + 1.2 \times 10^{-3}T^2$	$R^2 = 0.7848$	40
$dr = 1.33 \times 10^{-2} - 1.22 \times 10^{-2}\eta + 4 \times 10^{-3}T - 6.3 \times 10^{-3}\eta T + 1.26 \times 10^{-2}\eta^2 - 2.2 \times 10^{-3}T^2$	$R^2 = 0.6149$	41

1
2
3
4
5
6
7
8
9
10
11
12
13
14
15
16
17
18
19
20
21
22
23
24
25
26
27
28
29
30
31
32
33
34
35
36
37
38
39
40
41
42
43
44
45
46
47
48
49
50
51
52
53
54
55
56
57
58
59
60
61
62
63
64
65

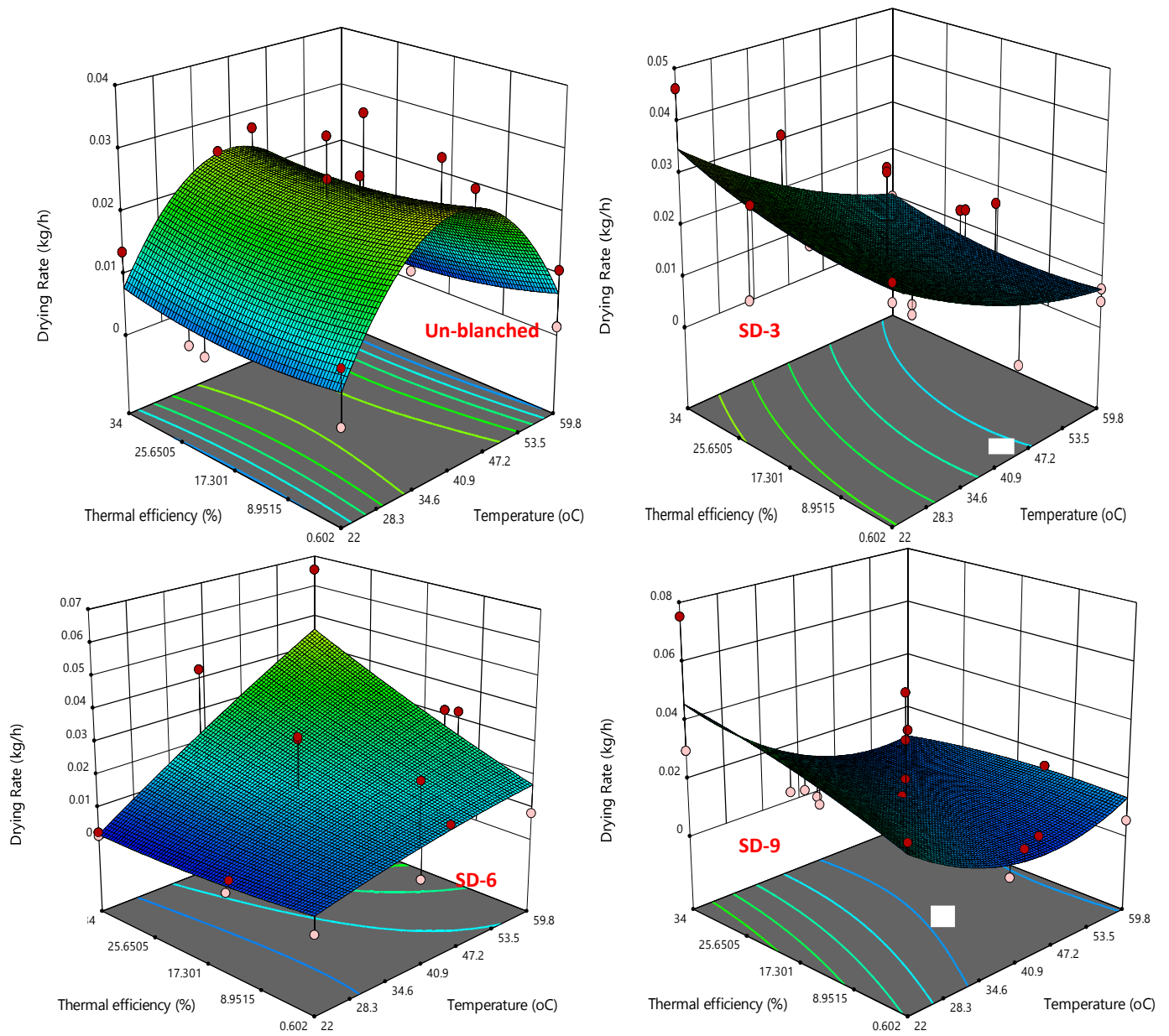


Figure 11: Surface plot of drying rate response to collector temperature and thermal efficiency variations

3.5.2 Mathematical modelling

The moisture content data was converted to a non – dimensional moisture ratio to predict the drying curve according to equation 33. The moisture ratio data were fitted with the drying time according to semi-theoretical and empirical diffusion equations presented in Table 3 to obtain the drying constants (k) and other arbitrary constants. Research has shown that these constants vary from product to product and are also affected by the drying methods, drying equipment used and treatment is given before the drying process (Hawa et al., 2021; Rabha et al., 2017). Table 4 shows the drying constants' values and other arbitrary constants obtained for each presented model in Table 3. As reported earlier, the constants and the statistical data were generated using a non-linear fitting algorithm in curve expert software. Validation of the models was based on the statistical data, as also presented in Table 4. The best-fitting model selected is the one with the highest R^2 , lowest root means square error (RMSE) and chi-square (χ^2) values. Therefore for all the pre-treatments, the allometric power function had the highest R^2 , lowest root means

square error (RMSE), and chi-square (χ^2) values except for sun drying of 6 minutes blanched and untreated potato where Wang and Singh's model had a better prediction. Therefore the allometric power function and Wang and Singh model were selected for predicting the moisture curve of blanched potato. In contrast, page and diffusion model was found to be a better predictor for solar drying of blanched turmeric (Nukulwar and Tungikar, 2021, Sharma et al., 2021). The fitting of the predicted and experimental values of the two thin layer models for each treatment is presented in Figure 12 with R^2 values of 0.9868 to 0.9992. However, the thin layer model for drying pre-treated potato slices in the solar dryer is presented in equations 42 to 45 for SD-3, SD-6, SD-9 and SD_u while equations 46 to 49 showed the thin layer model for drying under the sun for S₃, S₆, S₉ and S_u respectively. Although the allometric power function and Wang and Singh model had the best fitting, all the selected models had R^2 ranging from, 0.8493 - 0.99232, χ^2 values ranging from, 0.0008308 - 0.0196 and, RMSE values ranging from, 0.01329 - 0.60772.

Table 4: Model and statistical parameters for solar drying of potato slice.

Model	S ₃	S ₆	S ₉	S _u	SD-3	SD-6	SD-9	SD _u
Wang and Singh								
a	-0.0407	-0.04436	-0.04188	-0.0353	-0.0365	-0.0484	-0.0512	-0.03225
b	0.000164	0.0003125	0.000208	-0.00003	-0.00093	-0.0003	-0.0001	-0.00096
χ^2	0.00199	0.00284	0.00415	0.00537	0.00123	0.00235	0.00234	0.00131
RMSE	0.05774	0.08505	0.12451	0.16116	0.02097	0.03998	0.04207	0.02221
R^2	0.98291	0.97674	0.96802	0.96004	0.98793	0.98172	0.97978	0.98494
Page								
k	0.0657	0.0685	0.06725	0.06251	0.07395	0.08656	0.0865	0.06883
R^2	0.89815	0.90206	0.88044	0.8493	0.88206	0.88341	0.89975	0.8679
RMSE	0.34404	0.35815	0.46545	0.60772	0.20501	0.25495	0.2086	0.23654
χ^2	0.01147	0.01155	0.01501	0.0196	0.01139	0.01342	0.01098	0.01245
Logarithmic								
a	3.20701	2.0473	2.48098	5.08615	5.87539	8.41768	4.2743	3.4693
k	0.01399	0.02582	0.02043	0.00844	0.01016	0.00722	0.01492	0.01446
c	-2.1767	-0.98991	-1.4133	-4.0252	-4.8188	-7.3571	-3.2144	-2.4482
χ^2	0.00195	0.0026	0.00378	0.00502	0.00253	0.00277	0.00191	0.00191
RMSE	0.05473	0.0755	0.10581	0.14547	0.04041	0.0499	0.03252	0.03434
R^2	0.9838	0.97935	0.97146	0.96393	0.97674	0.97718	0.98437	0.98080
Henderson and Pabis								
a	1.1326	1.1562	1.1799	1.1787	1.1480	1.1654	1.1558	1.1385
k	0.073539	0.07785	0.07796	0.07237	0.08824	0.1027	0.1019	0.0815
R^2	0.9647	0.9688	0.9644	0.9469	0.9602	0.9597	0.9668	0.9506
RMSE	0.0897	0.0869	0.09983	0.1182	0.08932	0.09784	0.08685	0.9791
χ^2	0.00293	0.00367	0.00498	0.00611	0.00363	0.00365	0.00301	0.00241
Allometric power function								
a	0.95667	0.98147	1.02196	0.99234	1.0507	1.2283	1.14886	1.02445
b	-0.01342	-0.02131	-0.03521	-0.01459	-0.04246	-0.1673	-0.1137	-0.03238
C	1.25751	1.1127	0.98312	1.24234	1.08119	0.65752	0.77533	1.1456
χ^2	0.0018	0.00188	8.693E-4	0.00173	8.308E-4	0.00306	0.00159	0.00199
RMSE	0.04675	0.05274	0.02434	0.04852	0.01329	0.06114	0.02698	0.03574
R^2	0.98957	0.98969	0.99112	0.98411	0.99232	0.97659	0.98624	0.98305

1
2
3
4
5
6
7
8
9
10
11
12
13
14
15
16
17
18
19
20
21
22
23
24
25
26
27
28
29
30
31
32
33
34
35
36
37
38
39
40
41
42
43
44
45
46
47
48
49
50
51
52
53
54
55
56
57
58
59
60
61
62
63
64
65

$MR = 0.95667 - 0.01342t^{1.25751}$	$R^2 = 0.99$	42
$MR = 0.98147 - 0.02131t^{1.1127}$	$R^2 = 0.99$	43
$MR = 1.02196 - 0.03521t^{0.98312}$	$R^2 = 0.99$	44
$MR = 0.99234 - 0.01459t^{1.24234}$	$R^2 = 0.98$	45
$MR = 1.0507 - 0.04246t^{1.08119}$	$R^2 = 0.99$	46
$MR = 1 - 0.0484t - 0.0003t^2$	$R^2 = 0.98$	47
$MR = 1.14886 - 0.1137t^{0.77533}$	$R^2 = 0.98$	48
$MR = 1 - 0.03225t - 0.00096t^2$	$R^2 = 0.98$	49

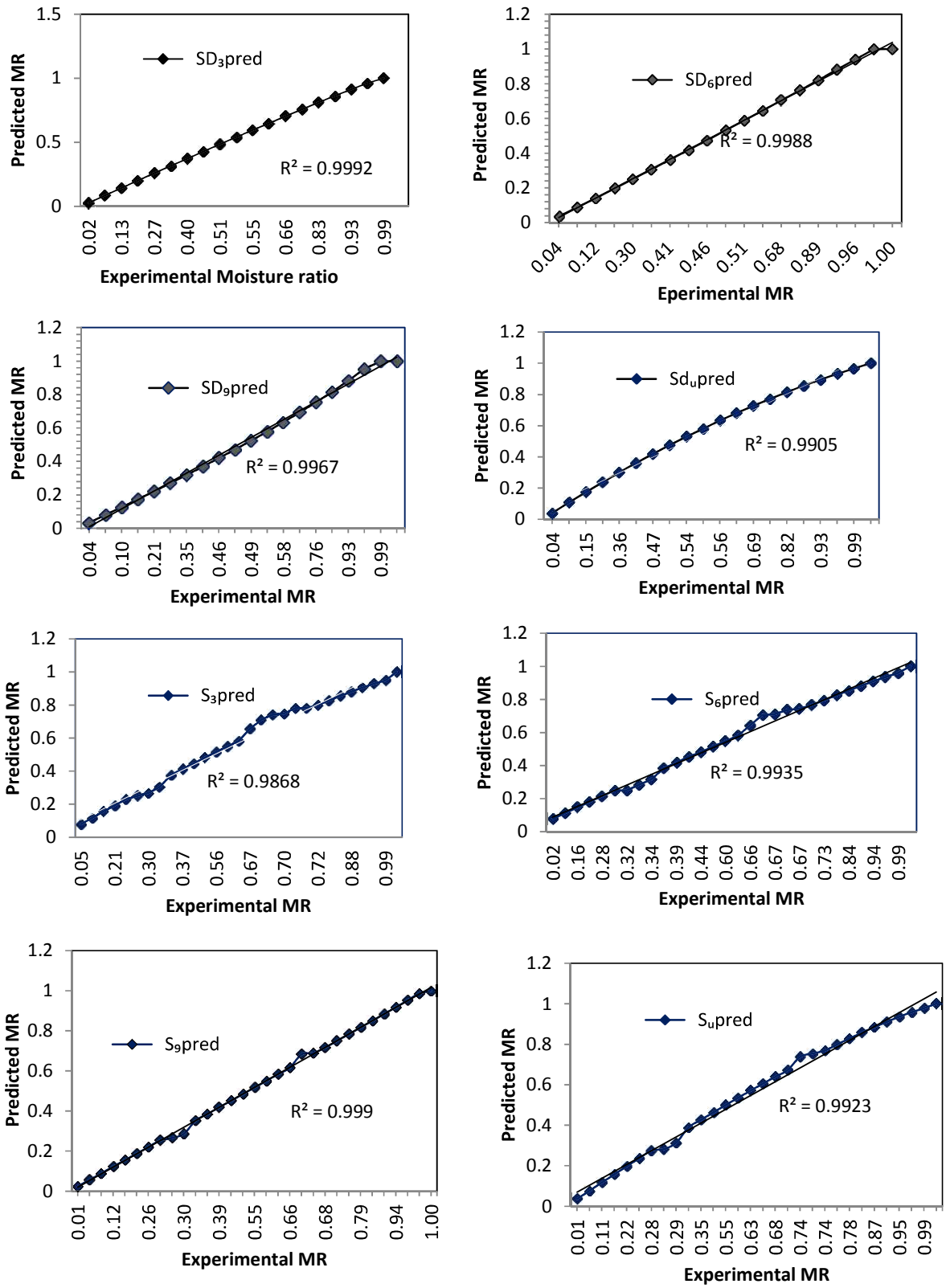


Figure 12: Experimental and predicted drying curve of the potato slices (S) sun (S.D.) Solar drying

3.5.3 Evolution of moisture diffusivity

The diffusivity evolution is presented in Figures 13 and 14 for sundried and solar-dried pre-treated potato slices, respectively. The moisture diffusivity was determined with equation 29, considering the time variation and radius of the potato slices as the product dries. The moisture diffusivity increased with a decrease in moisture content. However, this increase is not consistent due to the vagaries of weather that affect the heat transfer process. However, as the product loses moisture, the heat impact per moisture volume increases if the temperature value remains or increases within the existing thresholds, thus leading to higher heat transfer potential at that temperature threshold. Again according to Ndukwu et al., (2022e), during drying, the initial moisture transfer in agricultural products is driven by liquid diffusion. Still, as the dried product gains heat, the material expands and becomes more porous. At this period moisture transfer is driven by vapour diffusion. Therefore the moisture diffusivity increases with a decrease in moisture content as the time of drying increases. Other researchers have obtained a similar result (Agnihotri et al., 2016). Blanching time affected the effective moisture diffusivity as the values varied for different treatments. The effective moisture diffusivity for the pre-treated potatoes slices dried in the natural convection mix-mode solar dryer varied from 6.35×10^{-11} to $7.07 \times 10^{-10} \text{m}^2/\text{s}$ for sun-dried potato slices and 9.86×10^{-11} to $1.24 \times 10^{-9} \text{m}^2/\text{s}$ for solar drying of the same potato slices. This value is within the range obtained in literature for low-temperature drying of crops

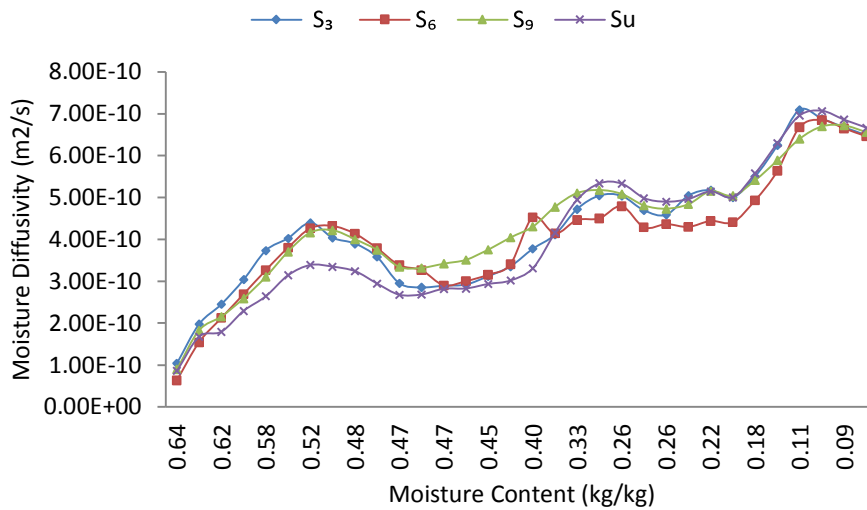


Figure 13: evolution of moisture diffusivity with moisture loss for sun-dried potato slices

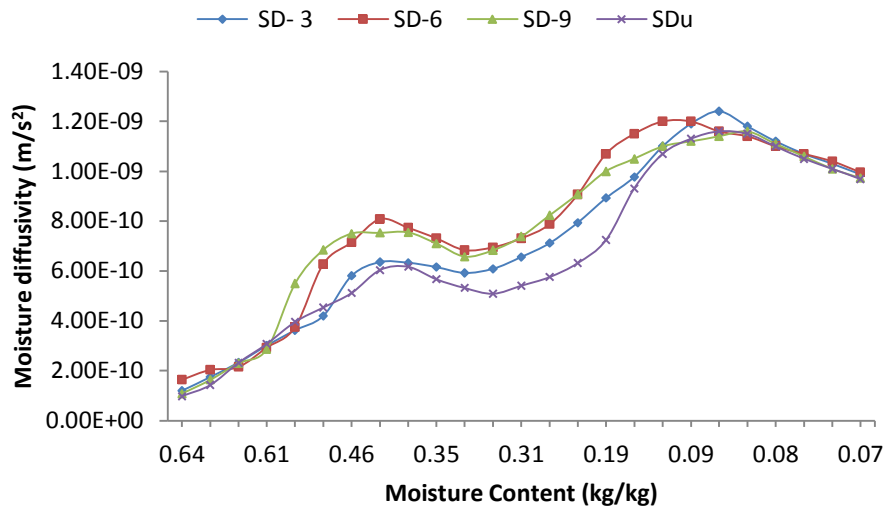


Figure 14: evolution of moisture diffusivity with moisture loss for solar-dried potato slices

4. Conclusion

In this research, the environmental impact, drying kinetics and optimization of the drying rate of blanched potato slices were investigated under natural convection mix-mode solar dryer and the sun. Drying of the potato slices from the initial moisture content of 64% w.b to the final moisture content of $7.85 \pm 0.64\%$ w.b took 20 to 31 h for drying in the solar dryer and under the sun. Blanching time affected the drying rate, and the optimum drying rate for the solar-dried untreated potato slices was determined as 0.0239665 kg/h at a collector temperature of 40.93°C and collector efficiency of 17.30% while blanching for 3 minutes, 6 minutes, and 9 minutes gave optimum drying rate of 0.0177959 kg/h , collector temperature (T) of 40.9°C thermal efficiency (η) of 17.30% for the three pre-treatments. The effective moisture diffusivity of the potato slices increased with a decrease in moisture content as the drying progressed. However, the solar dryer reduced the drying time from 25.81 to 34.48 % compared to open sun drying. The fitting of moisture ratio data with time using the thin layer equations showed that the Allometric 2 power function and Wang and Singh model can better predict the drying curve of blanched potato slices in the solar and under the sun drying. The thermal efficiency and energy utilization ratio were affected by weather parameters as they varied due to weather fluxes,. At the same time, coal powered dryer was deduced as the possible highest carbon emitter compared to other energy scenarios assessed if it is to be used to dry the potato slices instead of the presented solar dryer. However, the values of CO_2 that can be prevented (carbon mitigation) from entering the atmosphere range from 2.9 - 237.71 tonnes of CO_2 per year for all three energy scenarios assessed. The presented dryer can conserve energy and help poor farmers dry their crops more efficiently. The data generated can be used for improved design at optimum drying conditions.

Declarations

Funding

The authors Onyenwigwe Doris, Ndukwu Macmanus Chinenye, Abam Fidelis, Dirioha Cyprian and A.B.Eke acknowledge the support of the Tertiary Education Trust fund (TETFund) in sponsoring this project under the Education Research Fund(E.I.T./03/18).

Conflicts of interest/Competing interests

No conflict of interest existing among the contributors or institutions

1
2
3
4 **Availability of data and material**

5 All generated data for this publication is analyzed and included in this material.
6

7 **Code availability**

8 Not applicable
9

10 **Ethics of Approval**

11 Not applicable
12
13

14 **Consent to Participate**

15 Not Applicable
16
17

18 **Consent to Publish**

19 The authors confirm that the submitted work is not published, and the submission of the manuscript to J.B.E. is
20 approved by all authors with the consent to publish if accepted.
21
22
23
24
25
26

27 **References**

- 28
29 Ağbulut, Ü., Gürel, A.E., Biçen, Y., 2021. Prediction of daily global solar radiation using different
30 machine learning algorithms: Evaluation and comparison. *Renewable and Sustainable Energy*
31 *Reviews* 135, 110114
32 Agnihotri, V, A. Jantwal, R. JoshiG (2016).Determination of effective moisture diffusivity, energy
33 consumption and active ingredient concentration variation in *Inula racemosa* rhizomes during drying. *Ind.*
34 *Crops Prod.* (2016), <http://dx.doi.org/10.1016/j.indcrop.2016.09.068>
35
36 Alic E , Mehmet Das , Ebru Kavak Akpınar (2021).Design, manufacturing, numerical analysis and
37 environmental effects of single-pass forced convection solar air collector. *Journal of Cleaner Production*
38 311 (2021) 127518
39
40 Arun S., S. Ayyappan, V.V. Sreenarayanan (2014). Experimental studies on drying characteristics of
41 tomato in a solar tunnel greenhouse dryer, *Int. J. Rece. Technol. Eng.* (2014).
42 Arun K. R, S. Jayaraj (2021). Development and assessment of generalized drying kinetics in multi-tray
43 solar cabinet dryer. *Solar Energy* 226 (2021) 112–121
44
45 Azam M.M., M.A. Eltawil, B.M.A. Amer (2020). Thermal analysis of PV system and solar collector
46 integrated with greenhouse dryer for drying tomatoes, *Energy* 212 (2020), 118764,
47 <https://doi.org/10.1016/j.energy.2020.118764>.
48 Corrêa, P.C., Araújo, E.F. and Afonso Júnior, P.C. (2003). Determination of the parameters
49 related to thin-layer drying of sweet corn seeds (*Zea mays* L.]. *Rev. Bras. Milho e Sorgo.*
50 2:110-9.
51 Corrêa, P.C., Oliveira, G.H.H., Botelho, F.M., Goneli, A.L.D. and Carvalho, F.M. (2010).
52 Mathematical modelling and determination of the thermodynamic properties of coffee
53 (*Coffea arabica* L.) during the drying process. *Rev. Ceres.* 57:595-601.
54
55 Duffie J.A and Beckman W.A (2006) *Solar Engineering of Thermal Process*, Ed Wiley, New York
56
57
58
59
60
61
62
63
64
65

- 1
2
3
4
5 Esmaili, M., Sotudeh-Gharebagh, R., Cronin, K., Mousavi, M.A.E. and Rezazadeh, G. (2007) ‘Grape
6 drying: a review, *Food Reviews International*, Vol. 23, No. 3, pp.257–280.
- 7 El Hage, H., Herez, A., Ramadan, M., Bazzi, H., & Khaled, M. (2018). *An investigation on solar drying: A review*
8 *with economic and environmental assessment. Energy, 157, 815–829.* doi:10.1016/j.energy.2018.05.197
9 10.1016/j.energy.2018.05.197
- 10
11 ELkhadraoui A, S. Kooli, I. Hamdi, A. Farhat (2015). Experimental investigation and economic
12 evaluation of a new mixed-mode solar greenhouse dryer for drying red pepper and grape, *Renew.*
13 *Energy* (2015), <https://doi.org/10.1016/j.renene.2014.11.090>.
- 14
15 Forson, F. K., Nazha, M. A. A., Akuffo, F. O. and Rajakaruna, H. (2007). Design of Mixed-Mode Natural
16 Convection Solar Crop Dryers: Application of Principles and Rules of Thumb. *Journal of Renewable Energy*,
17 32(14): 2306–2319.
- 18
19 GPP. Nigeria Electricity Prices. Global Petrol Prices. 2021; pp. 1–5. Available online:
20
21 www.globalpetrolprices.com/Nigeria/electricity_prices/ (accessed on 15 May 2022)
- 22
23 Hawa L. C., U. Ubaidillah, S. A. Mardiyani, A. N. Laily, N. I. W. Yosika, and F. N. Afifah, “Drying kinetics of
24 cabya (*Piper retrofractum* Vahl) fruit as affected by hot water blanching under indirect forced convection
25 solar dryer,” *Sol. Energy*, vol. 214, no. December 2020, pp. 588–598, 2021.
- 26
27 Herez, A.; Khaled, M.; Murr, R.; Haddad, A.; Elhage, H.; Ramadan, M. Using Geothermal Energy for
28 cooling—Parametric study. *Energy Procedia* 2017, 119, 783–791.
- 29
30 Iheduwa V. E. · M. C. Ndukwu1 · U. C. Abada · I E. Ekop · L. Bennamoun · M. Simo- Tagne · F. I. Abam
31 (2022). Optimization of the energy consumption, drying kinetics and evolution of
32 thermo- physical properties of drying of forage grass for haymaking. *Heat and Mass Transfer*
33 <https://doi.org/10.1007/s00231-021-03146-2>
- 34
35
36 Jairaj, K.S., Singh, S.P., Srikant, K., 2009, A Review of Solar Dryers Developed for
37 Grape Drying, *Solar Energy*, 83, pp. 1698–1712.
- 38
39 Karthikeyan A.K., S. Murugavelh (2018).Thin layer drying kinetics and exergy analysis of turmeric
40
41 (Curcuma longa) in a mixed-mode forced convection solar tunnel dryer. *Renewable Energy* 128
42
43 (2018)
- 44
45 Kesavan, S., Arjunan, T.V., 2018. Experimental study on triple pass solar air heater with thermal energy
46 storage for drying mint leaves. *International Journal of Energy Technology and Policy* 14, 34-48.
- 47
48 Kirian, D.R. Principles of Economics and Management for Manufacturing Engineering; Elsevier Inc.:
49
50 Amsterdam, The Netherlands, 2022
- 51
52 Kumar S, M., A. Kumar, R. Kumar, H. Manchanda (2022). Comparison of groundnut drying in simple
53 and modified natural convection greenhouse dryers: thermal, environmental and kinetic
54 analyses, *J. Stored Prod. Res.* 98 (2022), 101990, <https://doi.org/10.1016/j.jspr.2022.101990>.
- 55
56
57
58 Lamrani B., Kuznik F., Ajbar A., Boumaza M. (2021) “Energy analysis and economic feasibility of

- wood dryers integrated with heat recovery unit and solar air heaters in cold and hot climates” *Energy* (228), 120598
- Lamrani B, Y. Elmrabet, M. Ibeh , N. Bekkioui, P. Etim , A. Chahboun, A. Draoui , M. C.Ndukwu (2022). *Energy*, economic analysis and mathematical modelling of mixed-mode solar drying of potato slices with thermal storage loaded V-groove collector: Application to Maghreb region. *Renewable Energy* 200 (2022) 48–58
- Lopez-Vida~na E.C, Caesar-Munguía Ana Lilia, García-Valladares Octavio ,Salgado Sandoval Orlando, Domínguez Ni~no Alfredo (2021).Energy and exergy analyses of a mixed-mode solar dryer of pear slices (*Pyrus communis* L), *Energy* 220 (2021) 119740S
- Milczarek, R R., J J. Ferry, F S. Alleyne, C W. Olsen, D A. Olson, R. Winston (2017). Solar thermal drum drying performance of prune and tomato pomaces.*Food and Bioproducts Processing*. <http://dx.doi.org/10.1016/j.fbp.2017.08.009>
- Murthy, M.V.R., 2009, A Review of New Technologies, Models and Experimental Investigations of Solar Driers, *Renewable and Sustainable Energy Reviews*, 13, pp. 835–844.
- Ndukwu M C, A.S. Ogunlowo, and O.J. Olukunle (2010). Cocoa Bean (*Theobroma Cacao* L.). Drying Kinetics. *Chil. J. Agr. Res. - Vol. 70 - Nº 4 – 633 – 639*.
- Ndukwu, M C , S I Manuwa (2015). A techno-economic assessment for the viability of some waste as cooling pads in evaporative cooling system *Int J Agric & Biol Eng. Vol. 8 No.2, 151 to 158*.
- Ndukwu M. C., Bennamou L., Abam F. I. (2018); Experience of solar drying in Africa: Presentation of designs, operations, and models. *Food Engineering. Review.*, 10, 211–244.
- Ndukwu, M. C., Onyenwigwe, D., Abam, F. I., Eke, A. B. and C, D. (2020a). Development of a low-cost wind-powered active solar dryer integrated with glycerol as thermal storage. *Renewable Energy*. doi:10.1016/j.renene.2020.03.016
- Ndukwu M. C., Diemuodeke E. O., Abam, F. I.; Abada, U. C., Eke- emezie N., Simo- Tagne M. (2020 b); Development and modelling of heat and mass transfer analysis of a low- cost solar dryer integrated with biomass heater: Application for West African Region.*Sci. Afr. 10*, e00615.
- Ndukwu, M. C., Bennamoun, L., Abam, F. I., Eke A. B., Ukoha D., (2017); Energy and exergy analysis of a solar dryer integrated with sodium
- Ndukwu M. C. and L. Bennamoun, (2018). Potential of integrating Na₂SO₄ · 10H₂O pellets in the solar drying system. *Dry. Technol.*, vol. 3937, 2018 b.
- Ndukwu, M.C.; Ibeh, M.; Ekop, I.; Abada, U.; Etim, P.; Bennamoun, L.; Abam, F.I.; Simo-Tagne, M.; Gupta, A (2022a). Analysis of the Heat Transfer Coefficient, Thermal Effusivity and Mathematical Modelling of Drying Kinetics of a Partitioned Single Pass Low-Cost Solar Drying of Cocoyam Chips with Economic Assessments. *Energies* 2022, 15, 4457. <https://doi.org/10.3390/en15124457>
- Ndukwu M. C, · Basseyy B. Okon · F. I. Abam · B. Lamrani · N. Bekkioui · H. Wu · L. Bennamoun · U. Egwu · C. N. Ezewuisi , C. B. Ndukwe · C. Nwachukwu · J. C. Ehiem. (2022b) *Energy and exergy analysis of solar dryer with triple air passage direction collector powered by a wind generator International Journal of Energy and Environmental Engineering*

1
2
3
4 <https://doi.org/10.1007/s40095-022-00502-8>
5

- 6 Ndukwu M.C., D. I Onyenwigwe, F. I. Abam, B. Lamrani, M. Simo-tagne, N. Bekkioui, L. Bennamoun, Z.
7 Said (2022c). Influence of hot water blanching and saline immersion period on the thermal
8 effusivity and the drying kinetics of hybrid solar drying of sweet potato chips, *Sol. Energy* 240
9 (2022) 176–192.
- 10 Ndukwu M. C., I. T. Horsfall, B. Lamrani, H. Wu, · L. Bennamoun, (2022d).Moisture evolution, thermal
11 properties and energy consumption of drying spent grain pellets from a blend of some cereals for
12 small- scale bio- energy utilization: modelling and experimental study. *Biomass Conversion and*
13 *Biorefinery*. <https://doi.org/10.1007/s13399-022-02846-x>
- 14 Ndukwu M.C., M.I. Ibeh, E.C. Ugwu, D.O. Igbojionu, A.A. Ahiakwo, Hongwei Wu (2022d).Evaluating coefficient
15 of performance and rate of moisture loss of some biomass humidifiers materials with a developed simple
16 direct stand-alone evaporative cooling system for farmers. *Energy Nexus* 8 (2022) 100146.
17 <https://doi.org/10.1016/j.nexus.2022.100146>
- 18
19
20
21 Nukulwar M.R, V. B. Tungikar (2021). Drying kinetics and thermal analysis of turmeric blanching and
22 drying using the solar thermal system. *Sustainable Energy Technologies and Assessments* 45 (2021)
23 101120
- 24
25 Ould-Amrouche, O., D. Rekioua, and A. Hamidat, Modelling Photovoltaic Water Pumping Systems and
26
27 Evaluation of their CO₂ Emissions Mitigation Potential. *Applied Energy* 87 (2010) 3451–3459.
28 doi:10.1016/j.apenergy.2010.05.021
- 29
30 Philip. N, S. Duraipandi, A. Sreekumar (2022). Techno-economic analysis of greenhouse solar dryer for
31
32 drying agricultural produce. *Renewable Energy*, 199, 613–627.
- 33
34 Rabha D.K., P. Muthukumar, C. Somayaji, (2017). Experimental investigation of thin layer drying
35 kinetics of ghost chilli pepper (*Capsicum Chinense* Jacq.) dried in a forced convection solar tunnel
36 dryer, *Renew. Energy* 105 (2017) 583e589.305e312
- 37
38 Rao V. V., S. P. Datta,(2020). A feasibility assessment of single to multi/hybrid evaporative coolers for
39
40 building air-conditioning across diverse climates in India, *Applied Thermal Engineering* 168
41 (2020) 14813
- 42
43
44 Sansaniwal S.K., M. Kumar, R.K. Sahdev, V. Bhutani, H. Manchanda (2022). Toward natural convection
45
46 solar drying of date palm fruits (*Phoenix dactylifera* L.): an experimental study, *Environ. Prog.*
47
48 *Sustain. Energy* (2022) 1–13, <https://doi.org/10.1002/ep.13862>.
- 49
50 Sekhar Y. R., A. K. Pandey, I.M. Mahbubul, G. R.Sai Avinash, V. Venkat, N. R. Pochont(2021).
51
52 Experimental study on drying kinetics for *Zingiber Officinale* using solar tunnel dryer with
53
54 thermal energy storage. *Solar Energy*, <https://doi.org/10.1016/j.solener.2021.08.011>
- 55
56 Sharma S, Dhalsamaant K, Tripathy PP, Manepally RK (2021). Quality analysis and drying
57
58 characteristics of turmeric (*Curcuma longa* L.) dried by hot air and direct solar dryers. *Lwt*
59
60 2021;138:110687.
- 61
62
63
64
65

- 1
2
3
4 Simo-Tagne, M., Ndukwu, M.C., Zoulalian, A., Bennamoun, L., Kifani-Sahban, F., Rogaume, Y., 2019.
5 Numerical analysis and validation of a natural convection mix-mode solar dryer for drying red
6 chilli under variable conditions, *Renewable Energy*, <https://doi.org/10.1016/j.renene.2019.11.055>.
7
8
9
10 Singh P, M.K. Gaur (2021b). Sustainability assessment of hybrid active greenhouse solar dryer
11 integrated with an evacuated solar collector. *Current Research in Food Science* 4 (2021) 684–691
12
13 Téllez M. C, I. P. Figueroa, B.C. Téllez, E. C. López Vidanab, A. L. Ortiz (2018). Solar drying of
14 Stevia (Rebaudiana Bertoni) leaves using direct and indirect technologies. *Solar Energy* 159 (2018) 898–907
15
16 Tiwari, S. Tiwari, G. N. (2017). Energy and exergy analysis of a mixed-mode greenhouse-type solar dryer,
17 integrated with partially covered N-PVT air collector. *Energy*, 128, 183–195.
18 doi:10.1016/j.energy.2017.04.022
19
20 Wang H. O., Q. Q. Fu, S. J. Chen, Z. C. Hu, and H. X. Xie (2018). “Effect of Hot-Water Blanching Pretreatment on
21 Drying Characteristics and Product Qualities for the Novel Integrated Freeze-Drying of Apple Slices,” *J.*
22 *Food Qual.*, vol. 2018.
23
24 Yassien, H.N.S., Alomar, O.R., Salih, M.M.M., 2020. Performance analysis of triple-pass solar air heater
25 system: Effects of adding a net of tubes below absorber surface. *Solar Energy* 207, 813-824
26
27 Yousef, M.S., Hassan, H., 2020. Energy payback time, exergoeconomic and enviroeconomic analyses of
28 using thermal energy storage system with a solar desalination system: an experimental study. *J. Clean.*
29 *Prod.* 270, 122082. <https://doi.org/10.1016/j.jclepro.2020.122082>
30
31 Xiong, Q., Hajjar, A., Alshuraiaan, B., Izadi, M., Altnji, S., & Shehzad, S. A. (2021a). State-of-the-art review of
32 nanofluids in solar collectors: A review based on the type of the dispersed nanoparticles. *Journal of Cleaner*
33 *Production*, 310, 127528. doi:10.1016/j.jclepro.2021.127528
34
35 Xiong, Q., Altnji, S., Tayebi, T., Izadi, M., Hajjar, A., Sundén, B., & Li, L. K. B. (2021b). A comprehensive review
36 on the application of hybrid nanofluids in solar energy collectors. *Sustainable Energy Technologies and*
37 *Assessments*, 47, 101341. doi:10.1016/j.seta.2021.101341
38
39
40 Zhang, M., Tang, J., Mujumdar, A.S., Wang, S., 2006, Trends in Microwave Related Drying of Fruits and
41 Vegetables, *Trends in Food Science & Technology*, 17, pp. 524-534
42
43
44
45
46
47
48
49
50
51
52
53
54
55
56
57
58
59
60
61
62
63
64
65